JOURNAL OF POROUS MEDIA

Volume 12, Number 11, 2009

CONTENTS

TECHNICAL NOTES

Journal of Porous Media (ISSN: 1091-028X) is published 12 times per year and is owned by Begell House, Inc, 50 Cross Highway, Redding, Connecticut 06896, Phone (203) 938-1300. USA subscription rate for 2009 is $961.00. Add $10.00 per issue for foreign airmail shipping and handling fees for all orders shipped outside the United States or Canada. All subscriptions are payable in advance. Subscriptions are entered on an annual basis, i.e., January to December. For immediate service and charge card sales, please call (203) 938-1300 Monday through Friday 9 AM — 5 PM EST. Orders can be faxed to (203) 938-1304 or mailed to Subscriptions Department, Begell House, Inc. 50 Cross Highway, Redding, Connecticut 06896.

Copyright © 2009 by Begell House, Inc. All rights reserved. Printed in the United States of America. Authorization to photocopy items for internal or personal use, or the internal or personal use of specific clients, is granted by Begell House, Inc. for libraries and other users registered with the Copyright Clearance Center (CCC) Transactional Reporting Service, provided that the base fee of $35.00 per copy, plus .00 per page is paid directly to CCC, 222 Rosewood Drive, Danvers, MA 01923, USA. For those organizations that have been granted a photocopy license by CCC, a separate system of payment has been arranged. The fee code for users of the Transactional Reporting Service is [ISSN 1091-028X/02 $35.00 + $0.00]. The fee is subject to change without notice.

Begell House, Inc.'s consent does not extend to copying for general distribution, for promotion, for creating new works, or for resale. Specific permission must be obtained from Begell House, Inc. for such copying.

This journal contains information obtained from highly regarded sources. Reprinted material is quoted with permission, and sources are indicated. A wide variety of references are listed. Reasonable efforts have been made to publish reliable data and information, but the editor and the publisher assume no responsibility for any statements of fact or opinion expressed in the published papers or in the advertisements.

Indexing and Abstracting: *Journal of Porous Media* is covered by several services provided by ISI®, including Current Contents®/ Engineering, Computing, and Technology, ISI Alerting Services™, and SCI, Science Citation Index®.

Printed October 16, 2009

Journal of Porous Media 12(11), 1083–1100 (2009)

Numerical Analysis of Natural Convection in Porous Cavities with Partial Convective Cooling Conditions

W. Pakdee* and P. Rattanadecho

Department of Mechanical Engineering, Faculty of Engineering, Thammasat University, Rangsit Campus, Klong Luang, Pathumtani 12120, Thailand

*E-mail: pwatit@engr.tu.ac.th and wpele95@yahoo.com

ABSTRACT

Transient natural convection flow through a fluid-saturated porous medium in a square enclosure with a partially cooling surface condition was investigated using a Brinkmann-extended Darcy model. The physical problem consists of a rectangular cavity filled with porous medium. The cavity is insulated, except the top wall that is partially exposed to an outside ambient. The exposed surface allows convective transport through the porous medium, generating a thermal stratification and flow circulations. The formulation of differential equations is nondimensionalized and then solved numerically under appropriate initial and boundary conditions using the finite difference method. The finite difference equations handling the convection boundary condition of the open top surface are derived for cooling conditions. In addition to the negative density gradient in the direction of gravitation, a lateral temperature gradient in the region close to the top wall induces the buoyancy force under an unstable condition. The two-dimensional flow is characterized mainly by the clockwise and anti-clockwise symmetrical vortices driven by the effect of buoyancy. The directions of vortex rotation generated under the cooling condition are in the opposite direction as compared to the heating condition. Unsteady effects of associated parameters were examined. The modified Nusselt number (Nu) was systematically derived. This newly developed form of Nu captures the heat-transfer behaviors reasonably accurately. It was found that the heat-transfer coefficient, Rayleigh number, Darcy number, as well as flow direction strongly influenced characteristics of flow and heat-transfer mechanisms.

Received June 11, 2008; Accepted September 8, 2008

Copyright © 2009 Begell House, Inc.

NOMENCLATURE

c_p	specific heat capacity [J/kg K]	β	coefficient of thermal expansion [1/K]
Da	Darcy number [-]	ε	porosity [-]
g	gravitational constant [m/s^2]	ς	dimensionless vorticity
h	convective heat-transfer coefficient [W/m^{2}K]	θ	dimensionless temperature
		κ	permeability of porous medium [m^2]
H	cavity length [m]	μ	dynamic viscosity [Pa/s]
k	thermal conductivity of the porous medium [W/m K]	ν	kinematic viscosity [m^2/s]
		ρ_f	fluid density [kg/m^3]
p	pressure [Pa]	τ	dimensionless time
Pr	Prandtl number [-]	ψ	stream function [m^2/s]
Ra	Rayleigh number [-]	Ψ	dimensionless stream function
t	time [s]	ω	vorticity [s^{-1}]
T	temperature [C]	**Subscripts**	
u, v	velocity component [m/s]	∞	ambient condition
x, y	Cartesian coordinates	e	effective
X, Y	dimensionless Cartesian coordinates	i	initial condition and index for a number of points in x direction
W	cavity width [m]		
Greek symbols		j	index for a number of points in y direction
α	thermal diffusivity [m^2/s]		

1. INTRODUCTION

The convective heating or cooling that causes heat and fluid flows inside a cavity is found in various applications including lakes and geothermal reservoirs, underground water flow, solar collectors, etc. (Bergman et al., 1986). Associated industrial applications include secondary and tertiary oil recovery, growth of crystals (Imberger and Hamblin, 1982), heating and drying processes (Stanish et al., 1986; Rattanadecho et al., 2001, 2002), electronic device cooling, solidification of casting, sterilization, etc. Natural or free convection in a porous medium has been studied extensively. Cheng (1978) provides a comprehensive review of the literature on free convection in fluid-saturated porous media with a focus on geothermal systems. Under the framework of porous media models, Darcy proposed the phenomenological relation between the pressure drop across a saturated porous medium and the flow rate. The Darcy model has been employed in recent investigations. Bradean et al. (1997) assumed Darcy's law and used a Boussinesq approximation to numerically simulatethe free convection flow in a porous media adjacent to a vertical or horizontal flat surface. The surface is suddenly heated and cooled sinusoidally along its length. The Darcy law with the Boussinesq approximationwas also employed by Bilgenand Mbaye (2001) to study the development of a Be'n-ard cell in a fluid-saturated porous cavity whose lateral walls were cooled. It was found that

the existence of two convective solution branches is related to the Darcy–Rayleigh and Biot numbers. Recently, a numerical study was conducted to solve the problem of thermosolutal convection within a rectangular enclosure (Bera and Khalili, 2002). The results revealed that anisotropy causes significant changes in Nusselt and Sherwood numbers. Many works of flow in porous media, such as the ones addressed above, have used the Darcy law. Although the Darcy law is applicable to slow flows, it does not account for initial and boundary effects. In the situation when the flow is strong and the solid boundary and viscous effects are not negligible, these effects, termed non-Darcy effects, become important (Khanafer and Chamkha, 1998). Bera et al. (1998) considered double diffusive convection due to constant heating and cooling on the two vertical walls based on a non-Darcy model inclined permeability tensor. Two distinguished modifications of Darcy' law are the Brinkmann and the Forchheimer extensions, which treat the viscous stresses at the bounding walls and the nonlinear drag effect due to the solid matrix, respectively (Nithiarasu et al., 1997). The Darcy–Forchheimer–Brinkman model was used to represent the fluid transport within the porous medium in the investigation of a convective flow through a channel (Marafie and Vafai, 2001). In this work the two-equation model was used to describe energy transport for solid and fluid phase. The Brinkman-extended Darcy model has been considered in the literature (Tong and Subramanian, 1985; Laurat and Prasad, 1987; Kim et al., 2000; Pakdee and Rattanadecho, 2006). The Darcy–Forchheimer model has been used in a number of published works (Beckermann et al., 1986; Lauriat and Prasad, 1989; Basak et al., 2006). In the study of effects of various thermal boundary conditions applied to saturated porous cavities, the conduction-dominant regime is within $Da \leq 10^{-5}$. Nithiarasu et al. (1998) examined the effects of the applied heat-transfer coefficient on the cold wall of the cavity upon flow and heat transfer inside a porous medium. The differences between the Darcy and non-Darcy flow regime are clearly investigated for different Darcy, Rayleigh, and Biot numbers and aspect ratios. Variations in Darcy, Rayleigh, and Biot numbers and aspect ratio significantly affect the natural flow convective pattern.

Natural convection flows with a variety of configurations were investigated for different aspects. Oosthuizen and Patrick (1995) performed numerical studies of natural convection in an inclined square enclosure with part of one wall heated to a uniform temperature and with the opposite wall uniformly cooled to a lower temperature and with the remaining wall portions. The enclosure is partially filled with a fluid and partly filled with a porous medium, which is saturated with the same fluid. The main results considered were the mean heat-transfer rates across the enclosure. Nithiarasu et al. (1997) examined effects of variable porosity on convective flow patterns inside a porous cavity. The flow was triggered by sustaining a temperature gradient between isothermal lateral walls. The variation in porosity significantly affected the natural flow convective pattern. Khanafer and Chamkha (1998) performed a numerical study of mixed convection flow in a lid-driven cavity filled with a fluid-saturated porous media. In this study, the influences of the Richardson number, Darcy number, and the Rayleigh number played an important role in mixed convection flow inside a square cavity filled with a fluid-saturated porous media. Recently, Al-Amiri (2000) performed numerical studies of momentum and energy transfer in a lid-driven cavity filled with a saturated porous medium. In this study, the force convection is induced by sliding the top constant-temperature wall. It was found that the increase in Darcy number induces flow activities, causing an increase in the fraction of energy transport by means of convection. With similar description of the domain configuration, Khanafer and Vafai (2002) extended the investigation to mass transport in the medium. The buoyancy effects that create the flow are induced by both temperature and concentration gradients. It was concluded that the influences of the Darcy number, Lewis number, and buoyancy ratio on thermal

and flow behaviors were significant. Furthermore, the state of the art regarding porous medium models has been summarized in recently published books (Nield and Bejan, 1999; Vafai, 2000; Pop and Ingham, 2001; Basak et al., 2006).

Previous investigations have merely focused on momentum and energy transfer in cavities filled with a saturated porous medium subjected to prescribed temperature and prescribed wall heat flux conditions. However, only a limited amount of numerical and experimental work on momentum and energy transfer in a cavity filled with a saturated porous medium subjected to heat-transfer coefficient boundary conditions at the exposed portion of the top wall has been reported. Moreover, very few published work is pertinent to partially heated or cooled porous media, although they are found in a number of applications, such as in flush-mounted electrical heaters or buildings (Desai et al., 1995; Al-Amiri, 2002; Oztop, 2007). The recent work of Oztop (2007) investigated natural convection in partially cooled and inclined porous enclosures. His study presented the steady-state results within the enclosure of isothermal heated and cooled walls. In our study, the surface is partially cooled under the convective boundary condition, allowing the surface temperature to change with time. The convective cooling condition or so-called condition of the third kind is systematically derived. While the focus of the present study is on the cooling effect, our recently published work (Pakdee and Rattanadecho, 2006) studied the influence of partially heated surfaces on thermal/flow behavior. In this previous work, although the results were qualitatively discussed in detail, no quantitative description of heat transfer in terms of Nusselt number (Nu) was reported. Therefore, in order to gain better insight into the analysis, our present study proposes a new formulation of Nu employed to analyze the heat-transfer behaviors. Moreover, to the best knowledge of the authors, no attention has been paid to transient convection due to surface partial convective cooling.

In the present study, the quantitative study in terms of Nu is taken into account. The new formulation of Nu is developed to correctly capture heat-transfer behaviors. The study of heat transfer due to cooling conditions has been carried out for transient natural convective flow in fluid-saturated porous medium filled in a square cavity. In contrast to the heating condition, the cooling condition changes the direction of the induced flows. The top surface is partially open to the ambient, allowing the surface temperature to vary depending on the influence of convection heat-transfer mechanism. Computed results are depicted using temperature, flow distributions, and heat-transfer rates in terms of local and average Nusselt numbers. The influences of associated parameters such as Rayleigh number and Darcy number on the flow and thermal configurations are examined.

2. PROBLEM DESCRIPTION

The computational domain depicted in Fig. 1 is a rectangular cavity of size W×H filled with a fluid-saturated porous medium. Aspect ratio of unity ($A = 1$) is used in the present study. The domain boundary is insulated except the top wall, which is partially exposed to an ambient air. The initial and boundary conditions corresponding to the problem are of the following forms:

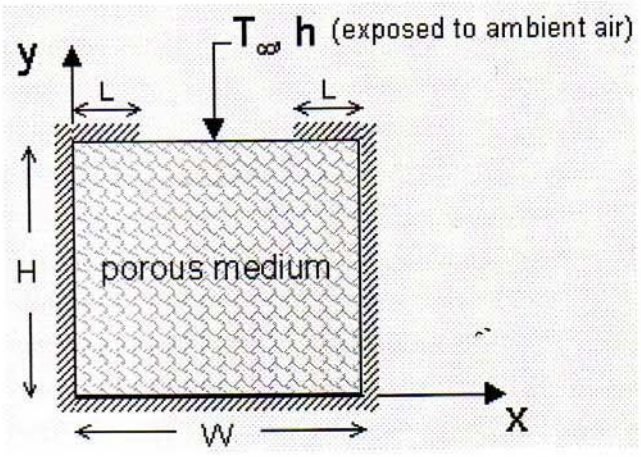

Figure 1. Schematic representation of the computational domain

$$u = v = 0, \quad T = T_i \quad \text{for} \quad t = 0 \tag{1}$$

$$\left.\begin{aligned} &u = v = 0 \ \text{ at } \ x = 0, \mathrm{W} \quad 0 \le y \le \mathrm{H} \\ &u = v = 0 \ \text{ at } \ y = 0, \mathrm{H} \quad 0 \le x \le \mathrm{W} \end{aligned}\right\} \tag{2}$$

$$\left.\begin{aligned} &\frac{\partial T}{\partial x} = 0 \ \text{ at } \ x = 0, \mathrm{W} \qquad 0 \le y \le \mathrm{H} \\ &\frac{\partial T}{\partial y} = 0 \ \text{ at } \ y = 0 \qquad\quad 0 \le x \le \mathrm{W} \\ &\frac{\partial T}{\partial y} = 0 \ \text{ at } \ y = \mathrm{H} \qquad\quad 0 \le x \le \mathrm{L} \\ &\text{and } \mathrm{W} - \mathrm{L} \le x \le \mathrm{W} \end{aligned}\right\} \tag{3}$$

The boundary condition at the exposed portion of the top wall is defined as

$$-k\frac{\partial T}{\partial y} = h[T - T_\infty] \quad \text{at} \quad y = \mathrm{H}$$
$$\mathrm{L} \le x \le \mathrm{W} - \mathrm{L} \tag{4}$$

where k and h are effective thermal conductivity and convection heat-transfer coefficient. This type of condition corresponds to the existence of convective heat transfer at the surface and is obtained from the surface energy balance.

The porous medium is assumed to be homogeneous and thermally isotropic. The saturated fluid within the medium is in a local thermodynamic equilibrium (LTE) with the solid matrix (El-Refaee et al., 1998; Nield and Bejan, 1999; Al-Amiri, 2002). The validity regime of local thermal equilibrium assumption has been established (Mohammad, 2000; Marafie and Vafai, 2001). The porous porosity is uniform. The fluid flow is unsteady, laminar, and incompressible. The pressure work and viscous dissipation are all assumed negligible. The thermophysical properties of the porous medium are taken to be constant. However, the Boussinesq approximation takes into account the effect of density variation on the buoyancy force, in which the fluid density is assumed constant except in the buoyancy term of the equation of motion. Furthermore, the solid matrix is made of spherical particles, while the porosity and permeability of the medium are assumed to be uniform throughout the rectangular cavity. Using standard symbols, the governing equations describing the heat-transfer phenomenon are given by

$$\frac{\partial u}{\partial x} + \frac{\partial v}{\partial y} = 0 \tag{5}$$

$$\frac{1}{\varepsilon}\frac{\partial u}{\partial t} + \frac{u}{\varepsilon^2}\frac{\partial u}{\partial x} + \frac{v}{\varepsilon^2}\frac{\partial u}{\partial y} = -\frac{1}{\varepsilon\rho_f}\frac{\partial P}{\partial x} + \frac{\upsilon}{\varepsilon}\left(\frac{\partial^2 u}{\partial x^2} + \frac{\partial^2 u}{\partial y^2}\right) - \frac{\mu u}{\rho_f \kappa} \tag{6}$$

$$\frac{1}{\varepsilon}\frac{\partial v}{\partial t} + \frac{u}{\varepsilon^2}\frac{\partial v}{\partial x} + \frac{v}{\varepsilon^2}\frac{\partial v}{\partial y} = -\frac{1}{\varepsilon\rho_f}\frac{\partial P}{\partial y} + \frac{\upsilon}{\varepsilon}\left(\frac{\partial^2 v}{\partial x^2} + \frac{\partial^2 v}{\partial y^2}\right) + g\beta(T - T_\infty) - \frac{\mu v}{\rho_f \kappa} \tag{7}$$

$$\sigma\frac{\partial T}{\partial t} + u\frac{\partial T}{\partial x} + v\frac{\partial T}{\partial y} = \alpha\left(\frac{\partial^2 T}{\partial x^2} + \frac{\partial^2 T}{\partial y^2}\right) \tag{8}$$

$$\sigma = \frac{[\varepsilon(\rho c_p)_f + (1-\varepsilon)(\rho c_p)_s]}{(\rho c_p)_f} \tag{9}$$

where κ is medium permeability, β is thermal expansion coefficient, α is effective thermal diffusivity of the porous medium, and μ and υ are viscosity and kinematic viscosity of the fluid, respectively. The symbols ε and ν denote the porosity of porous medium and fluid viscosity, respectively. In the present study, the heat capacity ratio σ is taken to be unity, because the thermal properties of the solid matrix and the fluid are assumed identical (Bergman et al., 1986; Khanafer and Vafai, 2002). The momentum equation consists of the Brinkmann term, which describes viscous effects due to the presence of a solid body (Brinkmann, 1947). This form of the momentum equation is known as the Brinkmann-extended Darcy model. Lauriat and Prasad (1987) employed the Brinkmann-extended Darcy formulation to investigate

the buoyancy effects on natural convection in a vertical enclosure. Although the viscous boundary layer in the porous medium is very thin for most engineering applications, inclusion of this term is essential for heat-transfer calculations (Al-Amiri, 2000). However, the inertial effect was neglected as the natural convection flow was studied (Basak et al., 2006).

The variables are transformed into the dimensionless quantities, defined as,

$$\left.\begin{aligned} X=\frac{x}{\mathrm{H}},\quad Y=\frac{y}{\mathrm{H}},\quad \tau=\frac{t\alpha}{\mathrm{H}^2},\quad U=\frac{u\mathrm{H}}{\alpha} \\ V=\frac{v\mathrm{H}}{\alpha},\quad \varsigma=\frac{\omega\mathrm{H}^2}{\alpha},\quad \Psi=\frac{\psi}{\alpha},\quad \theta=\frac{T-T_l}{T_h-T_l} \end{aligned}\right\} \quad (10)$$

where ω and ψ represent dimensional vorticity and stream function, respectively, and the symbol α denotes thermal diffusivity. Temperatures T_l and T_h change their values according to the problem type. In the heating case, T_l is initial temperature of a medium and T_h is an ambient temperature. In the other case of cooling, T_h is set to be an initial temperature of the medium, while T_l is an ambient temperature instead. The governing equations are transformed into a vorticity–stream function formulation. Thus, the dimensionless form of the governing equations can be written as

$$\frac{\partial^2\Psi}{\partial X^2}+\frac{\partial^2\Psi}{\partial Y^2}=-\varsigma \quad (11)$$

$$\varepsilon\frac{\partial\varsigma}{\partial\tau}+U\frac{\partial\varsigma}{\partial X}+V\frac{\partial\varsigma}{\partial Y}=\varepsilon\,\mathrm{Pr}\left(\frac{\partial^2\varsigma}{\partial X^2}+\frac{\partial^2\varsigma}{\partial Y^2}\right)+\varepsilon^2 Ra\,\mathrm{Pr}\left(\frac{\partial\theta}{\partial X}\right)-\frac{\varepsilon^2\,\mathrm{Pr}}{Da}\varsigma \quad (12)$$

$$\sigma\frac{\partial\theta}{\partial\tau}+U\frac{\partial\theta}{\partial X}+V\frac{\partial\theta}{\partial Y}=\alpha\left(\frac{\partial^2\theta}{\partial X^2}+\frac{\partial^2\theta}{\partial Y^2}\right) \quad (13)$$

$$\mathrm{U}=\frac{\partial\Psi}{\partial\mathrm{Y}},\quad \mathrm{V}=-\frac{\partial\Psi}{\partial\mathrm{X}} \quad (14)$$

where the Darcy number, Da, is defined as κ/H^2, and $\mathrm{Pr}=\nu/\alpha$ is the Prandtl number, where $\alpha=k_e/(\rho c_p)_f$ is the thermal diffusivity. The Rayleigh number Ra, which gives the relative magnitude of buoyancy and viscous forces, is defined as $\mathrm{Ra}=g\beta(T_i-T_\infty)\mathrm{H}^3/(\upsilon\alpha)$.

3. NUMERICAL PROCEDURE

The thermal properties of the porous medium are taken to be constant. Specific heat ratio of unity is assumed. The effective thermal conductivity of the porous medium considered is 10 W/m·K.

In the present study, the iterative finite difference method was used to solve the transient dimensionless governing equations [Eqs. (10)–(12)] subject to their corresponding initial and boundary conditions, given by Eqs. (1)–(4). Central–difference formulae were used for all spatial derivatives. The transient transport equations, Eqs. (12) and (13), were solved explicitly. A successive over-relaxation method (SOR) was utilized to solve for the flow kinematics relation given by Eq. (11). The velocity components, U and V, were computed according to Eq. (14). The approximation of convective terms is based on a second–order upwind finite differencing scheme, which correctly represents the directional influence of a disturbance. A uniform grid resolution of 61×61 was found to be sufficient for all smooth computations and computational time required in achieving steady-state conditions. Finer grids did not provide a noticeable change in the computed results.

3.1. Convective Cooling Boundary Condition

The finite difference form of boundary condition at the open part of the top surface was systematically derived based on the energy conservation principle. The boundary values of dimensionless temperature of a node i, j, and $\theta_{i,j}$ in the heating case are expressed as

$$\theta_{ij} = \frac{2\theta_{ij-1} + \theta_{i-1j} + \theta_{i+1j} + 2\dfrac{h\Delta y}{k}}{2\left(\dfrac{h}{k}\Delta Y + 2\right)} \tag{15}$$

where ΔY is the mesh size in y direction.

In the different case of cooling phenomenon, the expression is given by

$$\theta_{ij} = \frac{2\theta_{ij-1} + \theta_{i-1j} + \theta_{i+1j}}{2\left(\dfrac{h}{k}\Delta Y + 2\right)} \tag{16}$$

It can be noticed that both Eqs. (15) and (16) are independent of an ambient temperature T_∞, as it has been eliminated during the derivation. This feature is attractive since the solutions can be obtained regardless of a value of T_∞.

3.2. Corrected Formulation of Nusselt Number

The local Nusselt number (Nu) at the cooled horizontal surface is used as a tool to determine the ratio of convection heat transfer to conduction heat transfer within the porous enclosure. The accurate derivation of Nu is extremely important from the standpoint of determining the rate of heat transfer occurring at a surface. Based on the concept of energy balance at the surface for the cooling case,

$$-k \left.\frac{dT}{dy}\right|_{y=\mathrm{H}} = h(T_\mathrm{H} - T_\infty) \tag{17}$$

where H is indicated in Fig. 1 and with the definition of Nu,

$$\mathrm{Nu} = \frac{h\mathrm{H}}{k} = -\frac{\mathrm{H}}{(T_\mathrm{H} - T_\infty)} \left.\frac{dT}{dy}\right|_{Y=\mathrm{H}} \tag{18}$$

In terms of the dimensionless quantities θ and Y defined in the preceding Eq. (10), Nu will take the form

$$\mathrm{Nu} = -\frac{1}{\theta_\mathrm{H}} \left.\frac{d\theta}{dY}\right|_{Y=1} \tag{19}$$

where θ_H is the dimensionless temperature at the top surface.

The new formulation of Nu in the present work has not yet been found in the literature. This modified form of Nu takes into account temperature variation at the cooled surface. The average Nusselt number, $\overline{\mathrm{Nu}}$, is computed according to

$$\overline{\mathrm{Nu}} = \int_{\mathrm{L}}^{\mathrm{W-L}} \frac{\mathrm{Nu}(x)dx}{l} \tag{20}$$

where l is the length of the gap at the top wall.

In order to verify the accuracy of the present numerical study, the results obtained by the present numerical model were validated against the Benchmark solutions for natural convection in a cubic cavity (Wakashima and Saitoh, 2004). The comparisons tabulated in Table 1 reveal an excellent agreement within 1.5% difference. The present computed results were compared with those obtained by Aydin (2000) for free convection flow in a cavity, with a side-heated isothermal wall, filled with pure air (Pr = 0.7) for a Rayleigh number of 10^4. It was found that the solutions have good agreement with the previously published work. The results of selected tests are given in Table 2, which shows good agreement with the maximum value of the stream function and the maximum values of the horizontal and vertical velocity components between the present solution and that of Aydin. Moreover, the results from the present numerical model were compared with the solution of Nithiarasu et al. (1997) in the presence of porous medium for an additional source of confidence, as shown in Fig. 2 for streamlines and isotherms for which the compared contours have the same range of contour levels. The values Ra = 10^4, Da = 0.01, and $\varepsilon = 0.6$ were chosen. Table 3 clearly shows good agreement of the maximum values of the stream function and the vertical velocity component between the present solution and that of Nithiarasu et al (1997). All of these favorable comparisons lend confidence to the accuracy of the present numerical model.

Table 1

Comparison of the results obtained in the present study with those of the benchmark solutions for natural convection of air (Wakashima and Saitoh, 2004)

Ra	ω_{center}	Difference (%)	U_{max} (%)	Difference	V_{max} (%)	Difference
10^4 Present	1.111	0.82	0.202	1.51	0.220	0.2
Previous work	1.102		0.199		0.222	
10^5 Present	0.262	1.55	0.144	1.41	0.249	1.22
Previous work	0.258		0.142		0.246	

Table 2

Comparison of the results obtained in the present study with those of Aydin (2000)

	Present work	Published work	Difference (%)
ψ_{max}	5.070	5.087	0.33
U_{max}	16.300	16.225	0.46
V_{max}	19.730	19.645	0.43

Table 3

Comparison of the results obtained in the present study with those of Nithiarasu et al. (1997). (Da = 0.01, Ra = 10^4, porosity = 0.6)

	Present work	Published work	Difference (%)
ψ_{max}	2.53	2.56	1.17
V_{max}	9.49	9.34	1.60

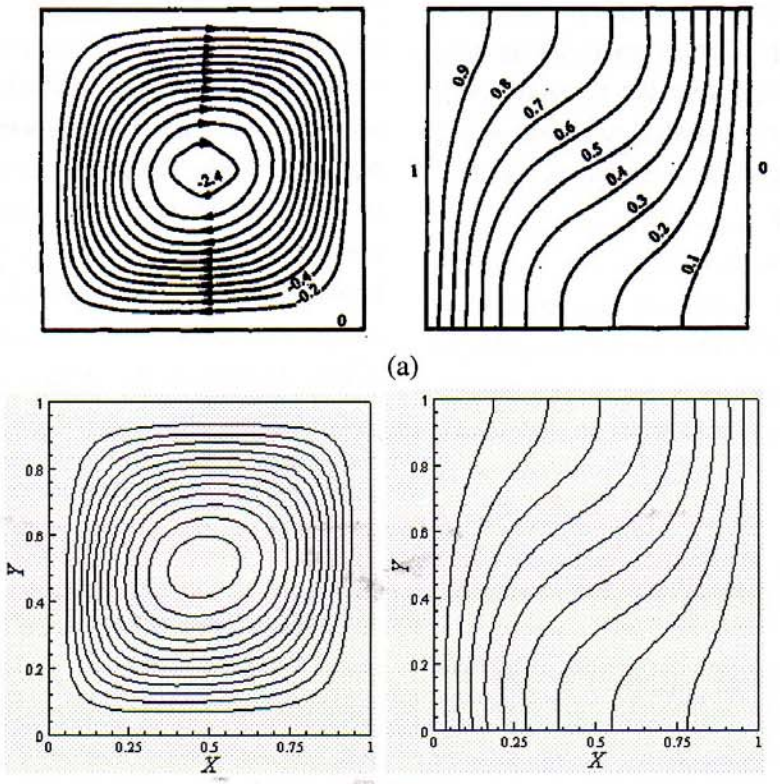

Figure 2. Test results for validation purposes: **(a)** Nithiarasu et al. (1997): non-Darcian model (including inertial and boundary effect), and **(b)** present simulation: Brinkman-extended Darcy model, which accounts for viscous effects

4. RESULTS AND DISCUSSION

The following discussions include the numerical results from the present study, which focuses on transient flow and thermal behaviors. Initial values of θ for an entire domain are set to 1 based on Eq. (10), as the ambient temperature is lower than the medium temperature in the cavity. The investigations were conducted for a range of controlling parameters, which are Darcy number (Da), Rayleigh number (Ra), and the convective heat-transfer coefficient (h). The uniform porosity ε of 0.8 and unity aspect ratio ($A = 1$) were considered throughout in the present study. In order to assess the global effects of these parameters, the streamlines and isotherm distributions inside the entire cavity are presented. All the figures have the same range of contour levels to facilitate direct comparisons.

The resulting computational fields were extracted at the time adequately long to ensure sufficient energy transferred throughout the domain. Figure 3 displays instantaneous images of the contour plots during the thermal and flow evolution. A Rayleigh number of 5×10^4, Da = 0.1, Pr = 1.0, h = 60 W/m^{2}K, and $\varepsilon = 0.8$ are considered. The two columns represent contours of temperature and stream function, respectively, from left to right. With the same contour levels, comparisons can be made directly. The four snapshots from top to bottom in each column are results taken at the dimensionless times $\tau = 0.013$, 0.088, 0.168, and 0.245. The vertical temperature stratification is observed. The streamline contours exhibit circulation patterns which are characterized by the two symmetrical vortices. The fluid flows as it is driven by the effect of buoyancy. This effect is distributed from the top wall of the cavity where the fluid is cooled through the partially open surface, causing lower temperature near the top boundary. The existence of the nonuniform temperature along the top surface and a decrease of density in the direction of gravitational force lead to an unstable condition. Thus, the buoyancy effect is associated with the lateral temperature gradients at locations near the top surface. High-temperature portions of fluid become lighter than the lower temperature portions at the middle where the wall is open. These light portions from two sides then expand laterally toward the center, compressing the lower temperature portions, which are heavier. As a result, the downward flows along the vertical centerline originate, while the lighter fluid rises, cooling as it moves. Consequently, the circulation flow pattern is generated. The clockwise and counter-clockwise circulations are located on the left side and right side, respectively, within the enclosure. The circulations get larger and expand downward with time. An increase in strength of the vortices develops fast during early simulation times, and its maximum magnitude reaches 6.0. Subsequently, the vortices are weakened. Similarly, temperature distribution progressively evolves relatively fast in the early times. Slow evolution is observed after that. This result corresponds well with the decrease in strength of flow circulations.

The resulting computational fields of the heating scenario are demonstrated in Fig. 4. For purposes of comparison, the parameter set remains unchanged. Similarly, the two columns represent temperature and stream function taken at the dimensionless times $\tau = 0.013$, 0.088, and 0.168. The vertical temperature stratification is observed. The streamline contours exhibit circulation patterns which are characterized by the two symmetrical vortices. The fluid flows as it is driven by the effect of buoyancy. This effect is distributed from the top wall of the cavity where the fluid is heated through the partially open area. Unlike the cooling case in which a presence of negative density mainly causes an unstable condition, in the heating case the lateral density gradient near the top surface is the only cause to the unstable condition that actually leads to the buoyancy force. This explains why the heated circulations are weaker than the cooled circulations presented earlier. Heated portions of the fluid become lighter than the rest of the fluid and are expanded laterally away from the center to the sides, then flow down along the two vertical walls, leading

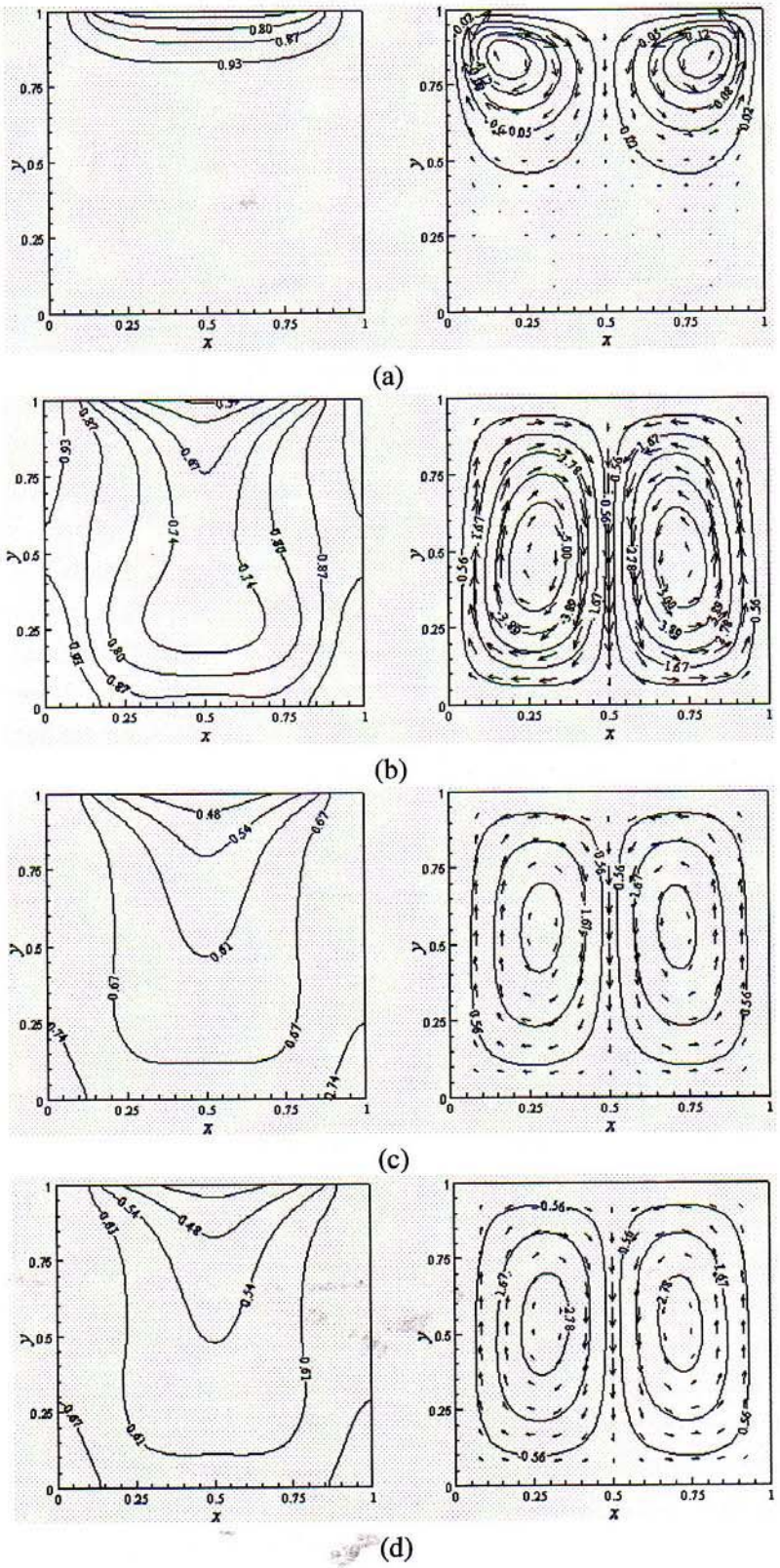

Figure 3. Sequential files with the cooling boundary for contours of temperature and streamlines at times τ = **(a)** 0.013, **(b)** 0.088, **(c)** 0.168, and **(d)** 0.245. ($Ra = 5 \times 10^4$, Da = 0.1, Pr = 1.0, $\varepsilon = 0.8$, and h = 60 W/m^{2}K)

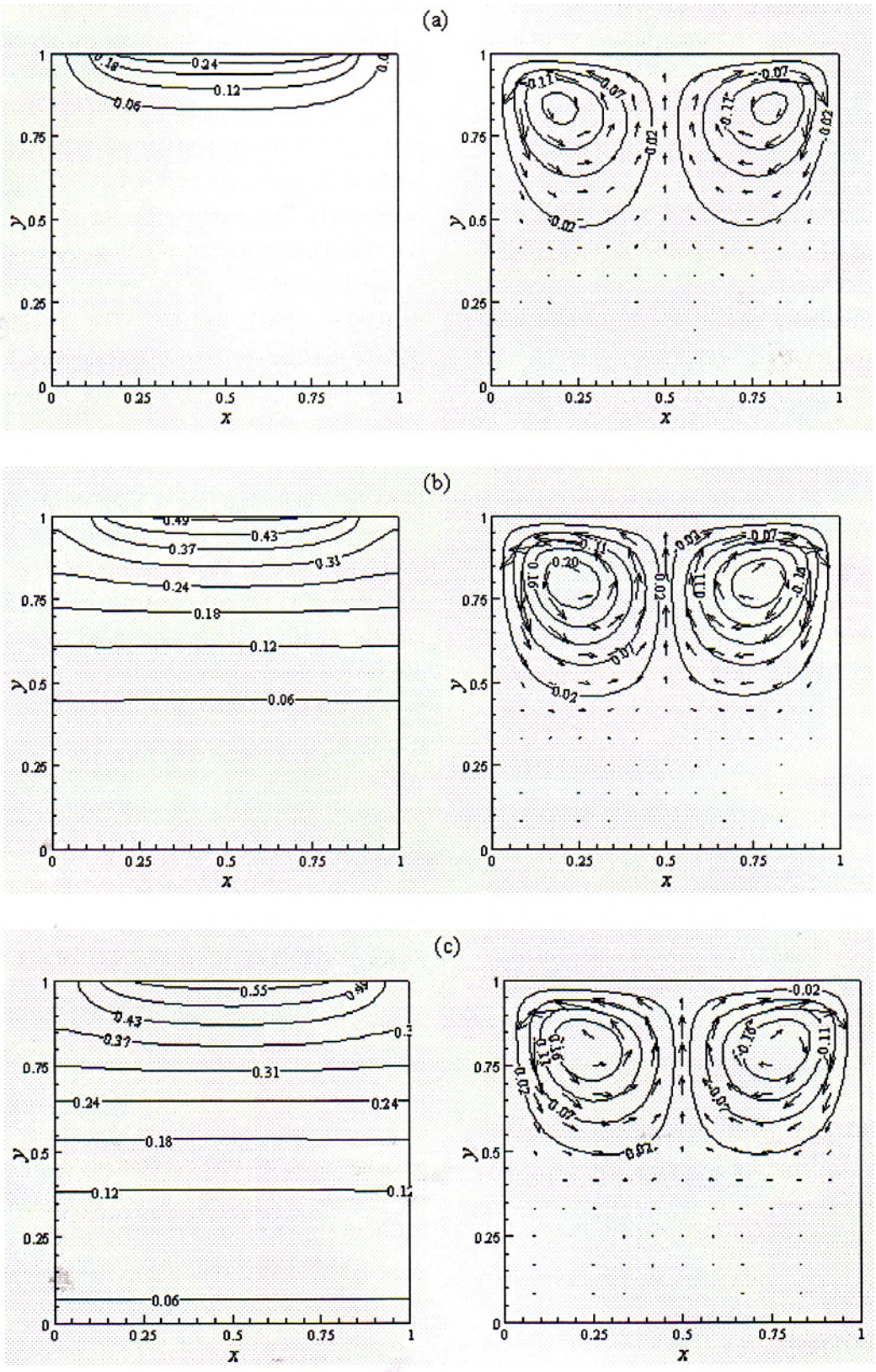

Figure 4. Sequential files with the heating boundary for contours of temperature and streamlines at times τ = **(a)** 0.013, **(b)** 0.088, and **(c)** 0.168. ($Ra = 5 \times 10^4$, $Da = 0.1$, $Pr = 1.0$, $\varepsilon = 0.8$, and $h = 60\ W/m^2K$)

to the counter-clockwise and clockwise flow circulations. These results suggest that the buoyancy forces are able to overcome the retarding influence of viscous forces. Note that directions of circulations are opposite to those under cooling condition. An increase in strength of the vortices develops fast during early simulation times and its maximum magnitude reaches 0.25, which is considerably small. Therefore, profiles of temperature contours look similar to those for a stationary fluid, in which the heat transfer is caused by conduction. Similarly, temperature distribution progressively evolves relatively fast in the early times. This result corresponds to the decrease in strength of flow circulations. In the remaining area, the fluid is nearly stagnant, suggesting that conduction is dominant due to minimal flow activities. This is because of prevailing viscous effects. It is evident from Figs. 3 and 4 that the cooling case provides a considerably faster thermal evolution and thereby greater convection rate. Furthermore, heat transfer in the vertical direction is much greater than that in the spanwise direction. The reader is directed to Pakdee and Rattanadecho (2006) for more detailed discussions of heating configuration.

Figure 5 shows the roles of Rayleigh number on the heat-transfer mechanism. The computed data was extracted at $\tau = 0.155$. Various Rayleigh numbers ($Ra = 5 \times 10^3$, 10^4, 5×10^4 and 10^5) are examined, whereas the Darcy number of 0.1, porosity of 0.8, and h of 60 W/m^2 K are fixed. The Rayleigh number provides the ratio of buoyancy forces to change in viscous forces. As Rayleigh number increases, the buoyancy-driven circulations inside the enclosure become stronger, as seen from greater magnitudes of stream function. For large Ra ($Ra = 5 \times 10^4$ and 10^5), contour lines of temperature penetrate faster relative to the low-Ra case, especially near the central locations. The result is more pronounced for larger Ra. This incident results from strong flow in the downward direction around the central domain. The downward flows assist heat to transfer toward the bottom of the enclosure. In contrast, near the vertical walls where the upward flows are present, the thermal propagation is hindered.

Effects of the Darcy number on the fluid flow and temperature inside the rectangular cavity are depicted in Fig. 6. The contour of isotherms and streamlines at $\tau = 0.155$ are plotted for different Darcy numbers, while ε, Pr, and h are kept at 0.8, 1.0, and 60 W/m^{2}K, respectively. Relatively high Ra of 5×10^4 is chosen. The Darcy number, which is directly proportional to the permeability of the porous medium, was set to 0.0001, 0.001, and 0.1. The case in which the porous medium is absent corresponds to an infinite Darcy number. The presence of a porous medium within the rectangular enclosure results in a force opposite the flow direction which tends to resist the flow, which corresponds to suppression in the thermal currents of the flow as compared to a medium with no pores (infinite Darcy number). It is evident that the increase in Da enhances the streamline intensities, thereby assisting downward flow penetration, which causes the streamline lines, i.e., two symmetrical vortices to stretch further away from the top surface. This results in expanding the region for which the convection significantly influences an overall heat-transfer process. Furthermore, the evolution results reveal a faster rate of vertical temperature distribution than the lateral rate. The results are consistent with the thermal behaviors observed in Fig. 5 for the same reasoning, which confirms how a flow direction impacts the convection heat transfer.However, as the Darcy number decreases, the flow circulations as well as thermal penetration are progressively retarded due to the reduced permeability of the medium. Figure 6(d) (Da = 0.0001) indicates that as the Darcy number approaches zero, the two circulations confined within the top domain appear very weak. In the remaining area the fluid is nearly stagnant with a very small temperature gradient, suggesting that conduction is dominant due to minimal flow activities.

Figure 7 presents how the average Nusselt number changes with time for a variety of Rayleigh numbers. The local Nu at the open portion on the top boundary

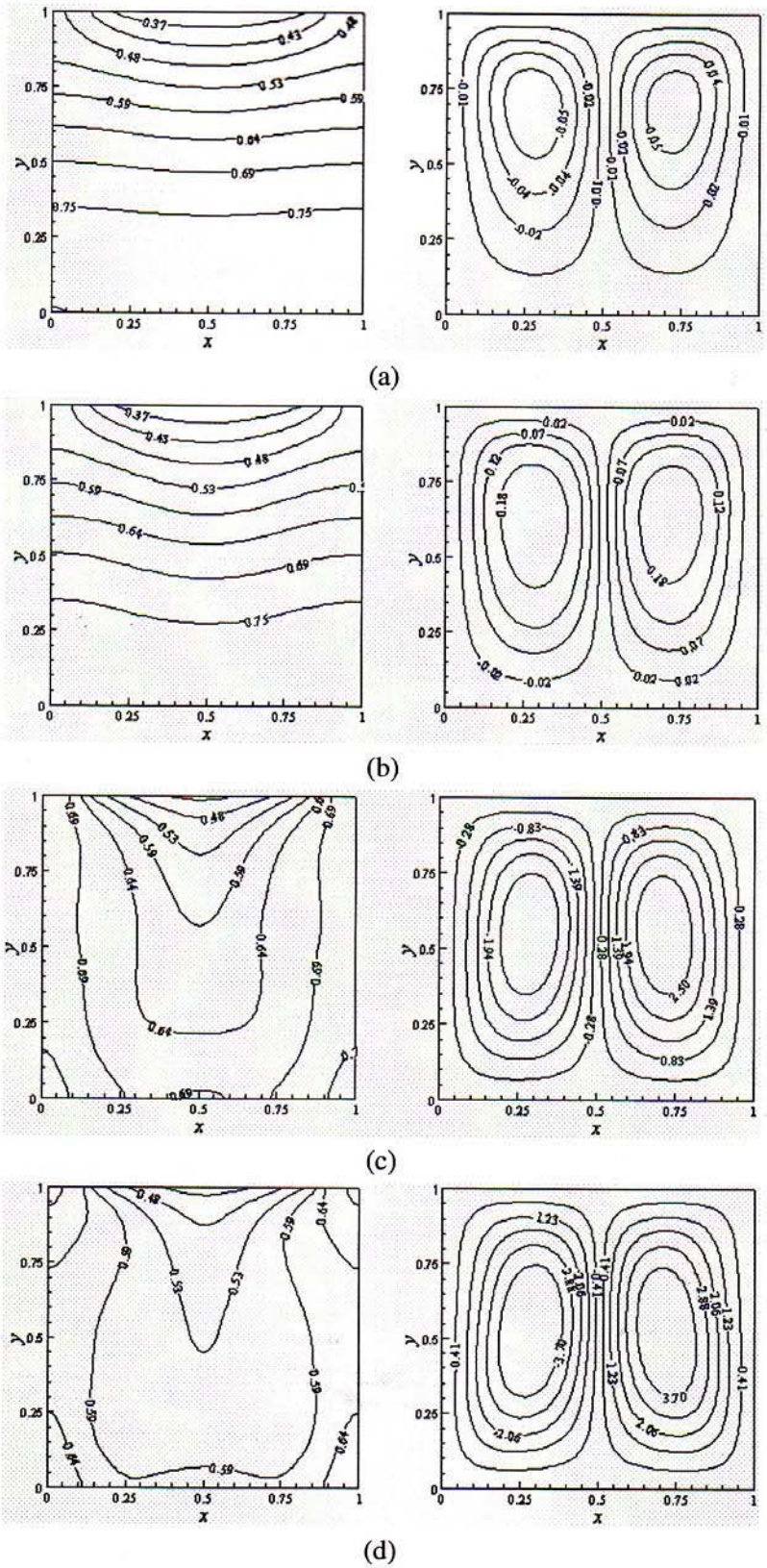

Figure 5. Contours of temperature and streamlines for the cooling case: **(a)** Ra = 5×10^3, **(b)** Ra = 10^4, **(c)** Ra = 5×10^4, and **(d)** Ra = 10^5. (Da = 0.1, h = 60 W/m^{2}K, Pr = 1.0, and $\varepsilon = 0.8$)

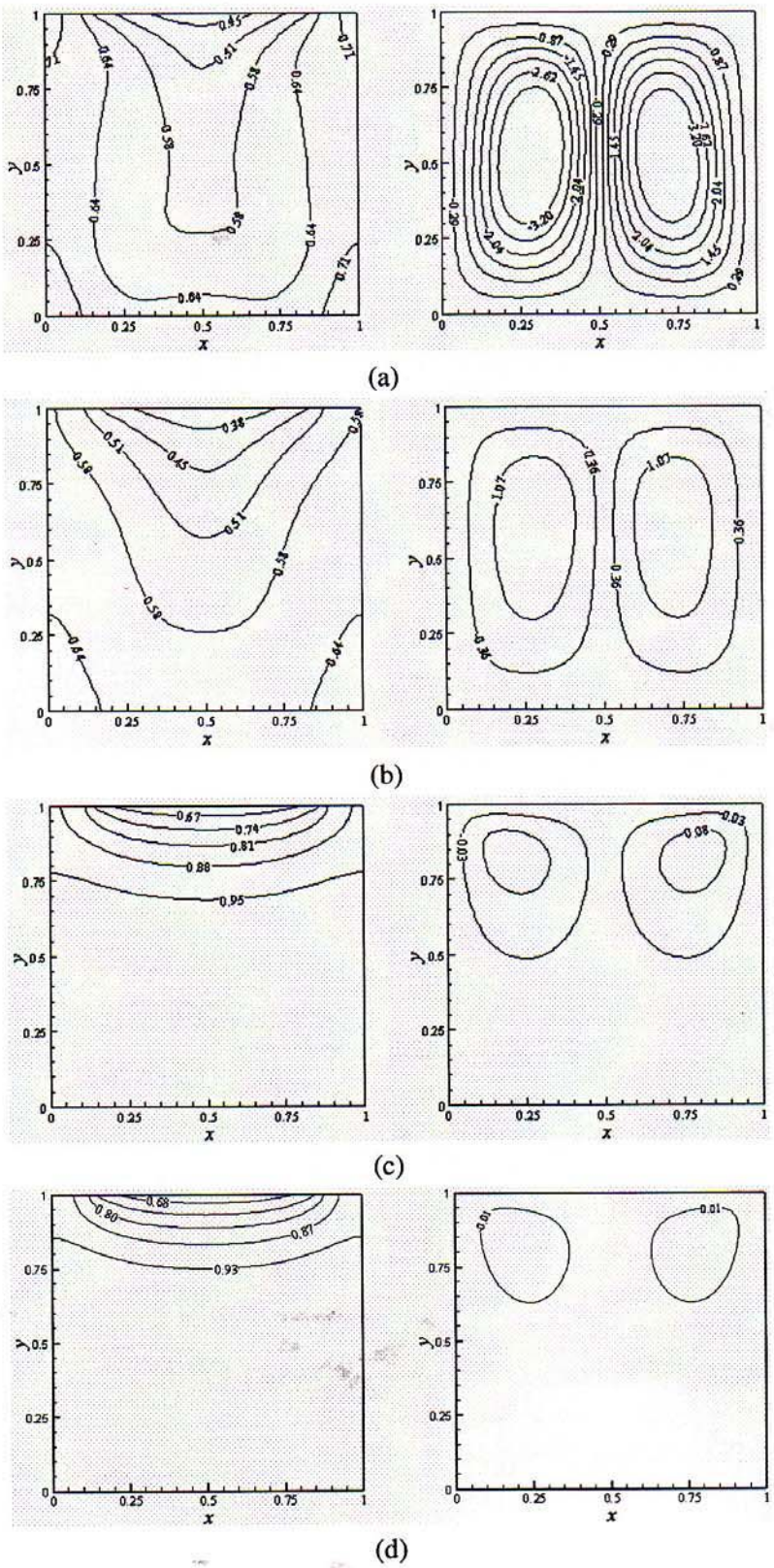

Figure 6. Contours of temperature and streamlines for the cooling case: **(a)** Da = infinity, **(b)** Da = 0.01, **(c)** Da = 0.001, and **(d)** Da = 0.0001. (Ra = 5×10^4, h = 60 W/m^{2}K, Pr = 1.0, and ε = 0.8)

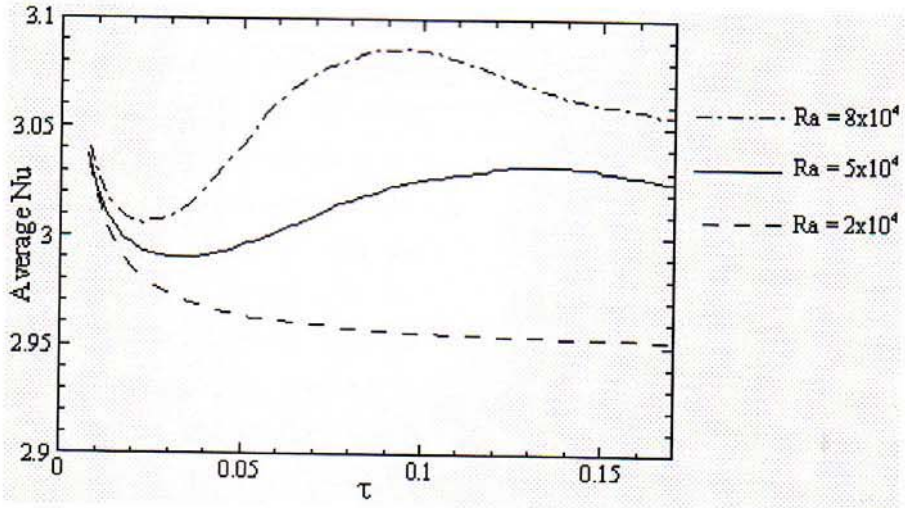

Figure 7. Variations of the average Nusselt number with time for different Rayleigh numbers. (Da = 0.01, h = 60 W/m^{2}K, Pr = 1.0, and $\varepsilon = 0.8$)

is computed according to Eq. (19). The average Nusselt number $\overline{\text{Nu}}$ is then obtained based on Eq. (20). Initially, the value of $\overline{\text{Nu}}$ decreases rapidly for all Rayleigh number values, clearly due to the fast reduction of temperature gradients. In the case of a low Rayleigh number of 2×10^4, $\overline{\text{Nu}}$ progressively decreases with time, while for higher Ra (5×10^4, 8×10^4), $\overline{\text{Nu}}$ values become greater and reach peak values after some time. By further increasing Ra (8×10^4), a higher maximum Nu is reached more quickly due to greater flow intensities. At late simulation times when a stable state is approached, the values of $\overline{\text{Nu}}$ continually decrease and essentially level off at late times, thereby diminishing heat transfer by means of heat convection. It can be expected that $\overline{\text{Nu}}$ will continue to decrease with time as the steady state is reached.

To gain insight into the observation made, the local values of the corresponding thermal and flow behaviors were traced for Ra of 8×10^4. The data are extracted and depicted in Fig. 8 at τ of 0.02, 0.1, and 0.16. The streamlines and isotherms are illustrated in Figs. 8a–c at $\tau = 0.02$, 0.1, and 0.16, respectively. At $\tau = 0.02$, the averaged Nu is small due to minimal flow activities. Then $\overline{\text{Nu}}$ gets higher as the flows gets stronger, which can be seen in Fig. 8b at $\tau = 0.1$. The effect of the rigorous flows overcomes the continual reduction of temperature gradient, resulting in the increase in $\overline{\text{Nu}}$. At the subsequent times, the viscous effect increasingly weakens the flows as shown in Fig. 8c. As a result, the reduction of temperature gradient prevails, causing $\overline{\text{Nu}}$ to decrease. These results correspond well with the variation of the averaged Nu with time, depicted in Fig. 7. The results confirm the validation of the proposed formulation of Nu.

To better understand the effects of Darcy number on the heat-transfer behavior, variations of $\overline{\text{Nu}}$ with time for different Darcy number are shown in Fig. 9. The resulting plots show interesting evidence of similar variations of $\overline{\text{Nu}}$ on Da and those on Ra, which was observed previously in Fig. 7 Average Nu correlates with Ra in a way similar to correlation of Nu with Da. Further increasing values of Da (0.05 and 0.1) cause larger $\overline{\text{Nu}}$ variations. Locations of the peak values are altered relative to Da value. A peak of profile is reached more quickly for higher Da. Greater Da gives higher $\overline{\text{Nu}}$, suggesting that the higher overall heat-transfer rate is due to more energetic vortices. However, $\overline{\text{Nu}}$ substantially reduces at late times.

5. CONCLUSIONS

Numerical simulations of natural convection flow through a fluid-saturated porous medium in a rectangular cavity due to cooling convection at the top surface were performed. Transient effects of asso-

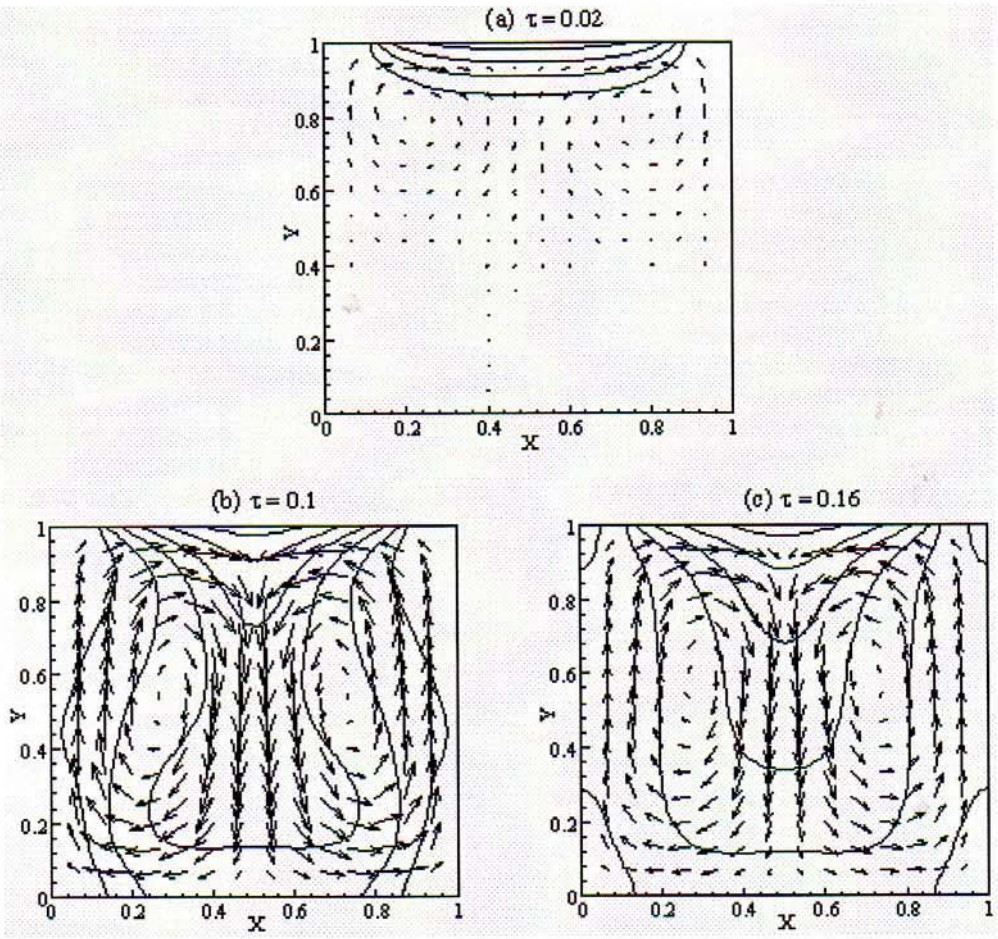

Figure 8. (a)–(c) Temperature contours overlaid by velocity vectors at $\tau = 0.02$, 0.1, and 0.16, respectively. Data is taken from that of Fig. 7 for $Ra = 8 \times 10^4$

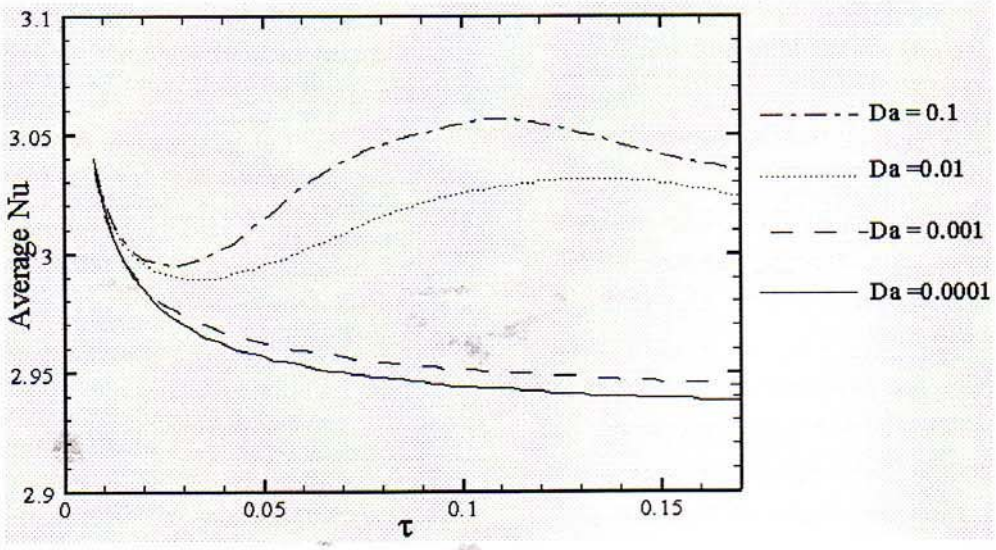

Figure 9. Variations of the average Nusselt number with time for different Darcy numbers. ($Ra = 5 \times 10^4$, h = 60 W/m^{2}K, Pr = 1.0, and $\varepsilon = 0.8$)

ciated controlling parameters were examined. The two-dimensional flow is characterized mainly by two symmetrical eddies that are initiated by the buoyancy effect. In the cooling case, the buoyancy effect is associated not only with the lateral temperature gradient at locations near the top surface, but also with the condition that the density gradient is negative in the direction of gravitational force. The buoyancy force is induced solely by the lateral temperature gradient in the heating case. The cooling and heating flow directions are opposite. Cooling flows are much stronger due to greater buoyancy effects, indicating higher overall convection rate. The heat-transfer mechanism is analyzed using the newly derived formulation of Nu. Heat-transfer rate is faster around a vertical symmetric line relative to the near-wall regions. Large Ra numbers increase streamline intensities, thus enhancing the downward flow penetration. The temperature stratification penetrates deeper toward the bottom wall and temperature range within the domain is extended. Therefore it enlarges the region where convection mode is significant. Small Darcy number values hinder the flow circulations. Therefore, heat transfer by convection is considerably suppressed. Furthermore, the new formulation of Nu captures the heat-transfer behaviors reasonably correctly. Interestingly, the dependences of Nu on Da and on Ra are found to have the same trends.

ACKNOWLEDGMENTS

This research was supported by the Thailand Research Fund (TRF) 2008 under contract no. MRG5180238.

REFERENCES

Al-Amiri, A. M., Analysis of Momentum and Energy Transfer in a Lid-Driven Cavity Filled with a Porous Medium, *Int. J. Heat Mass Transfer*, vol. **43**, pp. 3513–3527, 2000.

Al-Amiri, A. M., Natural Convection in Porous Enclosures: The Application of the Two-Energy Equation Model, *Numer. Heat Transfer, Part A*, vol. **41**, pp. 817–834, 2002.

Aydin, O., Determination of Optimum Air-Layer Thickness in Double-Pane Windows, *Energy Build.*, vol. **32**, pp. 303–308, 2000.

Basak, T., Roy, S., Paul, T., and Pop, I., Natural Convection in a Square Cavity Filled with Porous Medium: Effects of Various Thermal Boundary Conditions, *Int. J. Heat Mass Transfer*, vol. **49**, pp. 1430–1441, 2006.

Beckermann, C., Viskanta, R., and Ramadhyani, S., A Numerical Study of Non-Darcian Natural Convection in a Vertical Enclosure Filled with a Porous Medium, *Numer. Heat Transfer*, vol. **10**, pp. 557–570, 1986.

Bera, P., Eswaran, V., and Singh, P., Numerical Study of Heat and Mass Transfer in an Anisotropic Porous Enclosure Due to Constant Heating and Cooling, *Numer. Heat Transfer Part A*, vol. **34**, pp. 887–905, 1998.

Bera, P., and Khalili, A., Double-Diffusive Natural Convection in an Anisotropic Porous Cavity with Opposing Buoyancy Forces: Multi-Solutions and Oscillations, *Int. J. Heat Mass Transfer*, vol. **45**, pp. 3205–3217, 2002.

Bergman, T. L., Incropera, F. P., and Viskanta, R., Correlation of Mixed Layer Growth in Double-Diffusive, Salt-Stratified System Heated from Below, *J. Heat Transfer*, vol. **108**, pp. 206–211, 1986.

Bilgen, E., and Mbaye, M., Be'nard Cells in Fluid-Saturated Porous Enclosures with Lateral Cooling, *Int. J. Heat Fluid Flow*, vol. **22**, pp. 561–570, 2001.

Brinkmann, H. C., On the Permeability of Media Consisting of Closely Packed Porous Particles, *Appl. Sci. Res.*, vol. **1**, pp. 81–86, 1947.

Bradean, R., Ingham, D. B., Heggs, P. J., and Pop, I., The Unsteady Penetration of Free Convection Flows Caused by Heating and Cooling Flat Surfaces in Porous Media, *Int. J. Heat Mass Transfer*, vol. **40**, pp. 665–687, 1997.

Cheng, P., Heat Transfer in Geothermal Systems, *Adv. Heat Transfer*, vol. **4**, pp. 1–105, 1978.

Desai, C. P., Vafai, K., and Keyhani, M., On the Natural-Convection in a Cavity with a Cooled Top Wall and Multiple Protruding Heaters, *J. Electron. Packag.*, vol. **117**, pp. 34–45, 1995.

El-Refaee, M. M., Elsayed, M. M., Al-Najem, N. M., and Noor, A. A., Natural Convection in Partially Cooled Tilted Cavities, *Int. J. Numer. Methods*, vol. **28**, pp. 477–499, 1998.

Imberger, J., and Hamblin, P. F., Dynamics of Lakes, Reservoirs, and Cooling Ponds, *Ann. Rev. Fluid Mechanics*, vol. **14**, pp. 153–187, 1982.

Khanafer, K. M., and Chamkha, A. J., Mixed Convection Flow in a Lid-Driven Enclosure Filled with a Fluid-Saturated Porous Medium, *Int. J. Heat Mass Transfer*, vol. **42**, pp. 2465–2481, 1998.

Khanafer, K., and Vafai, K., Double-Diffusive Mixed Convection in a Lid-Driven Enclosure Filled with a Fluid-Saturated Porous Medium, *Numer. Heat Transfer, Part A*, vol. **42**, pp. 465–486, 2002.

Kim, S. J., Kim, D., and Lee, D. Y., On the Local Thermal Equilibrium in Microchannel Heat Sinks, *Int. J. Heat Mass Transfer*, vol. **43**, pp. 1735–1748, 2000.

Lauriat, G., and Prasad, V., Natural Convection in a Vertical Porous Cavity: A Numerical Study for Brinkmann-Extended Darcy Formulation, *ASME J. Heat Transfer*, vol. **109**, pp. 295–320, 1987.

Lauriat, G., and Prasad, V., Non-Darcian Effects on Natural Convection in a Vertical Porous Enclosure, *Int. J. Heat Mass Transfer*, vol. **32**, pp. 2135–2148, 1989.

Marafie, A., and Vafai, K., Analysis of Non-Darcian Effects on Temperature Differentials in Porous Media, *Int. J. Heat Mass Transfer*, vol. **44**, pp. 4401–4411, 2001.

Mohammad, A. A., Nonequilibrium Natural Convection in a Differentially Heated Cavity Filled with a Saturated Porous Matrix, *J. Heat Transfer*, vol. **122**, pp. 380–384, 2000.

Nield, D. A., and Bejan, A., *Convection in Porous Media*, New York: Springer, 1999.

Nithiarasu, P., Seetharamu, K. N., and Sundararajan, T., Natural Convective Heat Transfer in a Fluid Saturated Variable Porosity Medium, *Int. J. Heat Mass Transfer*, vol. **40**, pp. 3955–3967, 1997.

Nithiarasu, P., Seetharamu, K. N., and Sundararajan, T., Numerical Investigation of Buoyancy Driven Flow in a Fluid Saturated Non-Darcian Porous Medium, *Int. J. Heat Mass Transfer*, vol. **42**, pp. 1205–1215, 1998.

Oosthuizen, P. H., and Patrick, H., Natural Convection in an Inclined Square Enclosure Partly Filled with a Porous Medium and with a Partially Heated Wall, American Society Mechanical Engineers, Heat Transfer Division, HTD 302, pp. 29–42, 1995.

Oztop, H. F., Natural Convection in Partially Cooled and Inclined Porous Rectangular Enclosure, *Int. J. Thermal Sci.*, vol. **46**, pp. 149–156, 2007.

Pakdee, W., and Rattanadecho, P., Unsteady Effects on Natural Convective Heat Transfer through Porous Media in Cavity Due to Top Surface Partial Convection, *Appl. Thermal Eng.*, vol. **26**, pp. 2316–2326, 2006.

Pop, I., and Ingham, D. B., *Convective Heat Transfer, Mathematical and Computational Modeling of Viscous Fluids and Porous Media*, Oxford: Pergamon, 2001.

Ratanadecho, P., Aoki, K., and Akahori, M., A Numerical and Experimental Investigation of the Modeling of Microwave Drying Using a Rectangular Wave Guide, *J. Drying Technol.*, vol. **19**, pp. 2209–2234, 2001.

Ratanadecho, P., Aoki, K., and Akahori, M., Influence of Irradiation Time, Particle Sizes and Initial Moisture Content During Microwave Drying of Multi-Layered Capillary Porous Materials, *ASME J. Heat Transfer*, vol. **124**, pp. 151–161.

Wakashima, S., and Saitoh, T. S., Benchmark Solutions for Natural Convection in a Cubic Cavity Using the High-Order Time–Space Method, *Int. J. Heat Mass Transfer*, vol. **47**, pp. 853–864, 2004.

Stanish, M. A., Schager, G. S., and Kayihan, F., A Mathematical Model of Drying for Hygroscopic Porous Media, *AIChE J.*, vol. **32**, pp. 1301–1311, 1986.

Tong, T. W., and Subramanian, E., A Boundary-Layer Analysis for Natural Convection in Vertical Porous Enclosures, Use of the Brinkman-Extended Darcy Model, *ASME J. Heat Transfer*, vol. **28**, pp. 563–571, 1985.

Vafai, K., *Handbook of Porous Media*, New York: Marcel Dekker, 2000.